Soft Chemistry Routes to YPO_4-Based Phosphors: Dependence of Textural and Optical Properties on Synthesis Pathways

J. M. Nedelec,* D. Avignant, and R. Mahiou

Laboratoire des Matériaux Inorganiques, CNRS UMR 6002, Université Blaise Pascal, 24 Avenue des Landais, 63177 Aubiere Cedex, France

Received June 22, 2001

Different liquid routes have been used to prepare Eu^{3+}-activated YPO_4 phosphors. These materials have been compared with conventionally obtained YPO_4. For the first time (to our knowledge), a specific sol−gel approach has been developed to produce this material. All phases have been checked with X-ray diffraction (XRD) and solid-state nuclear magnetic resonance. Evaluation of the textural properties of the materials with XRD and scanning electron microscopy have demonstrated that the synthesis pathway can greatly influence the morphology of the materials and that in particular, the sol−gel route yields the smallest particles with the narrowest distribution. The optical study of the obtained phosphors shows that even if all materials exhibit comparable fluorescence in term of energetic scheme, some discrepancies can be noted according to the preparation route. In particular, liquid derived materials show shorter emission lifetimes; this observation has been correlated with residual OH groups in these materials. We have also observed that the emission yield, which is a fundamental parameter for applications purposes, depends on the preparation and that the coprecipitation technique leads to the best efficiency.

Introduction

Research on phosphors has always been very active. But some recent developments have given it a new boost. These developments include the use of alternative excitation sources such as plasma discharge for fluorescent lamps and displays (PDP).[1] In the first stage, classical materials have been used as phosphors for these applications regardless of the important differences in the conditions of excitation. Practical use of these materials has revealed several unexpected drawbacks such as short-term degradation, poor color quality, and a quick drop in luminous efficiency. Consequently, replacement solutions became necessary. Research in this way is more focused on the improvement of the existing phosphors[2] rather than the development of new ones. Among the various possibilities to improve phosphors, the synthesis pathway is probably the most important. Indeed, specific routes can lead to phosphors with controlled morphology and enhanced optical properties. Soft chemistry routes are particularly valuable to reach these objectives.

Most of phosphor materials are based on oxides doped either with rare earth ions or transition metal ions. Among these oxides, the family RMO_4, where R = trivalent lanthanide or Y and M = V, P, or As, is particularly interesting.[3−9] A good example is the use of Nd^{3+}-activated YVO_4 for lasing action in the IR region (∼1.06 μm). The compound YPO_4 belongs to this family and is the subject of the present work.

Yttrium orthophosphate crystallizes with the zircon structure (xenotime type) with a tetragonal symmetry ($a = b = 6.822$ and $c = 6.018$ Å) and space group I_1/amd. The structure can be described, as shown in Figure 1, as chains parallel to the c axis of corner-sharing structural units built of a (YO_8) dodecahedron and a (PO_4) tetrahedron[10] linked together by an edge. These chains are further linked together by edge sharing.

The europium orthophosphate $EuPO_4$ crystallizes with the monazite type, but partial substitution of Eu^{3+} for Y^{3+} does not affect the xenotime structure of YPO_4. YPO_4 materials doped with rare earths are of particular interest in the the production of luminescent materials. The aim of this work is to produce Eu^{3+}-activated YPO_4 phosphors and determine how the synthesis pathway can influence the textural and optical properties of the

* To whom correspondence should be addressed. E-mail: jnedelec@chimtp.univ-bpclermont.fr. Present address: Laboratoire des Matériaux Inorganiques UMR 6002, Université Blaise Pascal, 24 Avenue des Landais, 63 177 Aubière Cedex, France.

(1) Ballato, J.; Lewis, J. S., III; Holloway, P. *MRS Bull.* **1999**, *24*, 51.
(2) Fouassier, C. *Curr. Opin. Solid State Mater. Sci.* **1997**, *2*, 231.
(3) Ropp, R. C. *Luminescence and the solid state*; Elsevier: New York, 1991.
(4) Antic-Fidancec, E.; Hölsa, J.; Lemaitre-Blaise, M.; Porcher, P. *J. Phys.*: *Condens. Matter* **1991**, *3*, 6829.
(5) Becker, J.; Gesland, J. Y.; Kirikova, N.; Krupa, J. C.; Makhov, V. N.; Runne, M.; Queffelec, M.; Uvarova, T. V.; Zimmerer, G. *J. Alloys Compd.* **1998**, *275−277*, 205.
(6) Huignard, A.; Gacoin, T.; Boilot, J. P. *Chem. Mater.* **2000**, *12*, 1090.
(7) Lian, R.; Yin, M.; Zhang, W.; Lou, L.; Krupa, J. C. *J. Alloys Compd.* **2000**, *311*, 97.
(8) Schwarz, L.; Finke, B.; Kloss, M.; Rohmann, A.; Sasum, U.; Haberland, D. *J. Lumin.* **1997**, *257*, 7274.
(9) Rambadu, U.; Amalnerkar, D. P.; Kale, B. B.; Buddhudu, S. *Mater. Chem. Phys.* **2001**, *70*, 1.
(10) Milligan, W. O.; Mullika, D. F.; Beall, G. W.; Boatner, L. A. *Acta Crystallogr.* **1983**, *39*, 23.

10.1021/cm010572y CCC: $22.00
Published on Web 01/30/2002

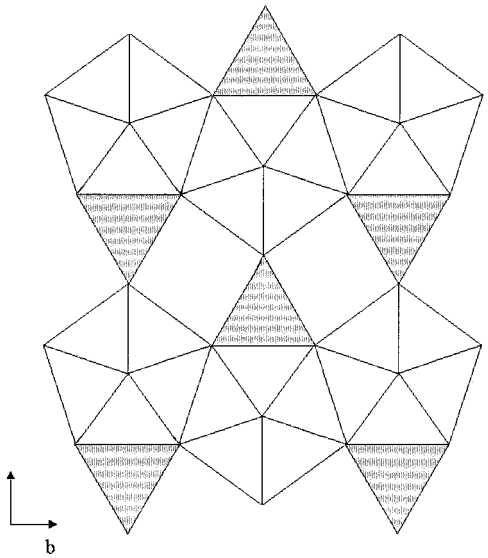

Figure 1. Projection of (PO_4) tetrahedra and (YO_8) dodecahedra on the (b,c) plane.

resulting red-emitting materials. Several routes have been used to synthesize Eu^{3+}-doped YPO_4 materials including a new sol−gel approach, previously unreported to the best of our knowledge. The preparation procedures will be described in the following section.

Experimental Section

Preparation of Materials. *Solid-State Preparation.* In comparison with soft chemistry routes, YPO_4 was first prepared by a classical solid-state reaction. The samples were prepared from a stoichiometric mixture of yttrium oxide, Y_2O_3, and ammonium dihydrogenophosphate, $(NH_4)H_2PO_4$, heated at 600 °C for 24 h. The resulting solid was then annealed at 1200 °C for 12 h, with these conditions for the final treatment being applied for all preparation methods. For Eu-doped materials, a mixture of europium and yttrium oxides was used and the amount of Eu^{3+} was fixed at 5% and kept constant throughout the whole study.

Three liquid routes were then used to prepare the orthophosphate.

Coprecipitation. A 0.1 M yttrium nitrate solution was added dropwise with stirring to a 0.1 M K_3PO_4 solution. YPO_4 precipitation occurs at a basic pH and with a large excess of potassium phosphate. Doping is achieved by the addition of europium nitrate (5%). The precipitate is then filtered, washed thoroughly with de-ionized water, and annealed at 1200 °C for 12 h.

Attack with H_3PO_4. Phosphoric acid is added directly to yttrium oxide (or a mixture of Y_2O_3 and Eu_2O_3 for doped materials). The mixture is then refluxed for 8 h, and the solution is filtered. The solid residue is washed with water and annealed at 1200 °C for 12 h.

Sol−Gel Method. We report here for the first time to our knowledge, an all-alkoxide sol−gel route to YPO_4. Phosphorus and yttrium alkoxides are formed in situ by the reaction of a 2-propanolate solution with P_2O_5 and YCl_3. The 2-propanolate is produced by the reaction of metallic potassium with 2-propanol. For doped materials, a mixture of YCl_3 and $EuCl_3$ was used. The sol thus obtained evolves quickly toward a white gel, which is separated by centrifugation and washed thoroughly to eliminate KCl resulting from the formation of the alkoxides. This amorphous gel is then annealed at 1200 °C for 12 h.

Characterization. *X-ray Diffraction* (*XRD*). XRD patterns were recorded on a Siemens D5000 powder diffractometer using the Bragg−Brentano configuration and the Cu Kα radiation (λ = 1.5406 Å).

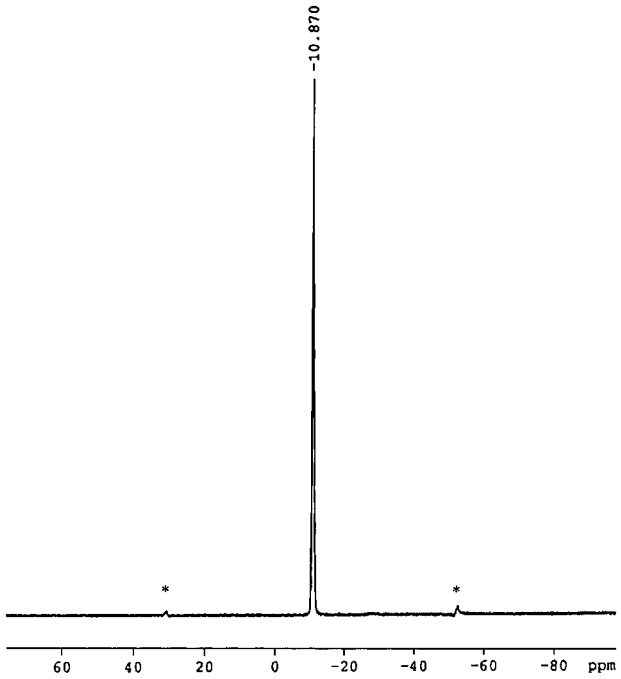

Figure 2. ^{31}P solid-state MAS NMR spectrum obtained for the coprecipitated sample. * spinning bands.

Solid-State Nuclear Magnetic Resonance (*NMR*). NMR spectra were recorded at room temperature on a Bruker MSL 300 solid-state NMR spectrometer at a magnetic field of 7.05 T, using double-bearing magic angle spinning 4 mm zirconia rotors. ^{31}P MAS NMR spectra were recorded at the frequency of 121.495 MHz. A spinning rate of 10 kHz was used with an initial pulse of 1.8 μs, 64 scans, and recycle delay time of 600 s.^{31}P chemical shifts were referenced to 85% H_3PO_4 (negative shifts correspond to high field).

Luminescence Measurements. Emission and excitation spectra were recorded at 15 K with a single monochromator Jobin Yvon HR 100 spectrometer and by using a ND62 Continuum dye laser pumped by a frequency doubled pulsed Continuum Surelite I Nd^{3+}:YAG laser. A mix of Rhodamine 590 and 610 was used for the dye solution. To achieve excitation in the $^5D_2$ level (blue), the dye laser beam was upshifted by stimulated Raman scattering in a high-pressure H_2 cell (shift 4155 cm^{-1}).

Time-resolved emission was monitored with an EG & G Boxcar, and fluorescence lifetimes were measured with a LeCroy 400 MHz oscilloscope.

Relative emission efficiencies were determined at room temperature under UV excitation at 254 nm with a filtered Xe lamp by integration of the emission spectra in the $^5D_0 \rightarrow {}^7F_2$ region and comparison with commercial Y_2O_3:Eu^{3+} 4.47%.

Results

All powders obtained after annealing at 1200 °C following the four synthesis procedures depicted previously were checked by solid-state MAS NMR and XRD. Figure 2 shows the typical MAS NMR spectrum obtained for our samples. This spectrum shows a single narrow peak with a chemical shift of −10.87 ppm confirming the production of very pure xenotime type YPO_4. The X-ray powder patterns obtained for the four undoped samples are identical and correspond to a single YPO_4 tetragonal phase. A diffractogram of a 5% Eu^{3+}-doped powder is displayed in Figure 3 and shows that for this low doping level, the xenotime structure is retained without any $EuPO_4$ monazite phase.

It can be inferred from NMR and XRD investigations that all synthesis pathways, including the newly devel-

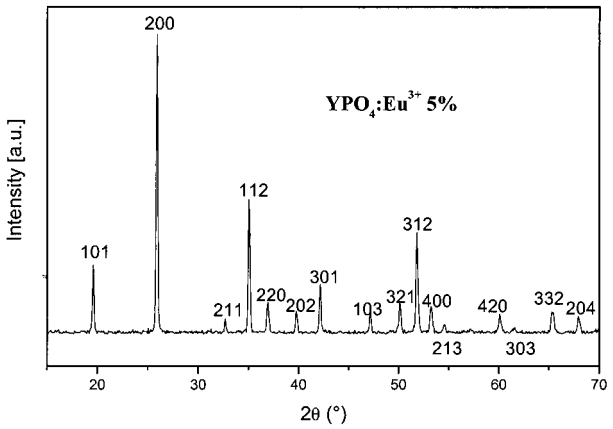

Figure 3. XRD pattern obtained for sol−gel derived doped sample with YPO_4 xenotime structure.

Table 1. Grain Size (Å) Derived from Laue−Scherrer Analysis of (200) XRD Peak

solid state	sol−gel	coprecipitation	acidic attack
819 ± 18	744 ± 19	927 ± 15	841 ± 4

oped sol−gel procedure, lead to a single crystallized phase YPO_4 of xenotime type.

Grain Size Measurements. XRD patterns have been recorded for the most intense peak (200) with a step scan of 0.01°. The Laue−Scherrer law[11] relates the position and width of the diffraction peak to the average grain size Φ according to the relation

$$\Phi = \frac{0.9\lambda}{\cos\theta_m\sqrt{(\epsilon^2 - \epsilon_0^2)}} \quad (1)$$

where λ is the wavelength of the radiation used (λ = 1.5406 Å), θ_m is the angle corresponding to the maximum of the peak, ϵ is the full width at half-maximum (fwhm), and ϵ_0 is the experimental beam aperture. To determine ϵ_0, the XRD pattern of well-crystallized quartz was used. The XRD peak was fitted with a Voigt function; this procedure was repeated several times to get information on the relative errors in the measurements. The results are displayed in Table 1 along with incertitude values.

SEM pictures recorded for two selected samples are shown in Figure 4. Extreme samples in term of grain size have been chosen: sol−gel and solid state for small and large grains, respectively. Samples resulting from coprecipitation and acidic attack lie somewhere between the latter two samples. These results confirm XRD results and clearly show that the sol−gel process lead to homogeneous powder with small particles (0.25 μm) with a narrow size distribution. The solid-state reaction on the contrary yields large particles (from 0.25 to 2 μm) with a large distribution. Coprecipitated and acidic attack derived powders have intermediate morphology.

Optical Study of Eu^{3+}-Doped Materials. The Eu^{3+} ion exhibits two main advantages: first, because of its simple and well-documented luminescence scheme, it serves as a very efficient and sensitive structural probe[12,13] and second, its luminescence, in the case of a non-centrosymmetric environment, is generally dominated by the $^5D_0-^7F_2$ transition yielding a red-emitting phosphor suitable for lamps and displays.

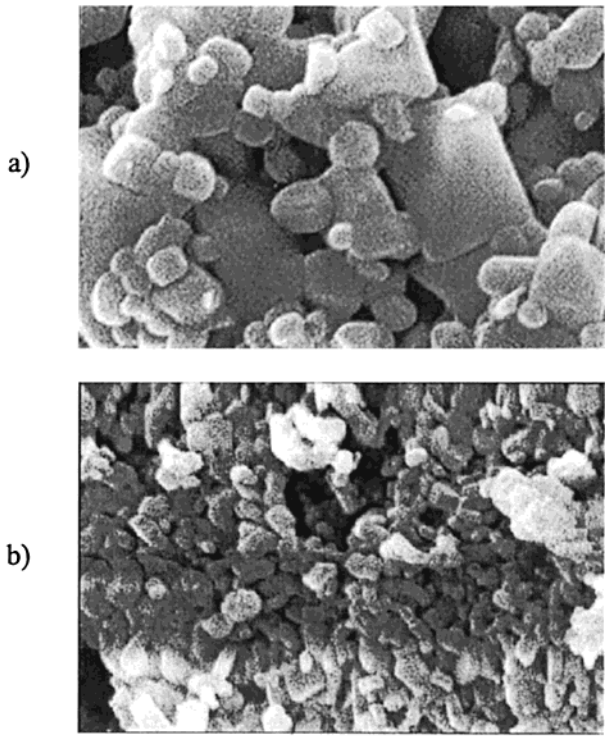

× 20 000

Figure 4. SEM obtained with a ×20 000 magnification for the solid state (a) and the sol−gel (b) derived samples.

In the first experiment, low-temperature (15 K) excitation spectra of Eu^{3+} in YPO_4 prepared by the different methods were recorded. Excitation in both the $^5D_0$ and the $^5D_2$ levels was performed by using the appropriate dye and H_2 cell for blue excitation. Excitation of the forbidden $^7F_0-^5D_0$ transition leads to a spectrum where small satellites can be detected as sidebands and where the maximum of the transition is located at around 578.5 nm in all compounds. The peaks of the satellites were connected to impurities (OH, rare earth ions, etc.) which are well-known to reduce nonequivalent crystallographic sites. For blue excitation ($^5D_2$), similar spectra consisting of two bands are obtained for all samples as shown in Figure 5. The most intense band peaking at about 466.6 nm was then selected to excite Eu^{3+} luminescence and record it. The spectra thus obtained at 15 K are displayed in Figure 6. All spectra are similar for the various samples, showing the $^5D_0-^7F_J$ (J = 1, 2, 4) transitions. Very intense $^5D_0-^7F_1$ transition yields a red-orange global luminescence. Precise measurements of the positions of the peaks do not show any significant variation for the different samples.

To complete the optical study of the materials, lifetimes of the $^5D_0-^7F_2$ fluorescence after excitation in the $^5D_0$ and $^5D_2$ levels were measured at 15 K. Excitation in the $^7F_0-^5D_0$ band leads to a purely exponential decay curve as shown in Figure 7a. Excitation in the

(11) Warren, B. E. *X-ray diffraction*; Dover Publications Inc.: New York, 1990.

(12) Campostrini, R.; Carturan, G.; Ferrari, M.; Montagna, M.; Pilla, O. *J. Mater. Res.* **1992**, *7*, 745.

(13) Lochhead, M. J.; Bray, K. L. *J. Non-Cryst. Solids* **1994**, *170*, 143.

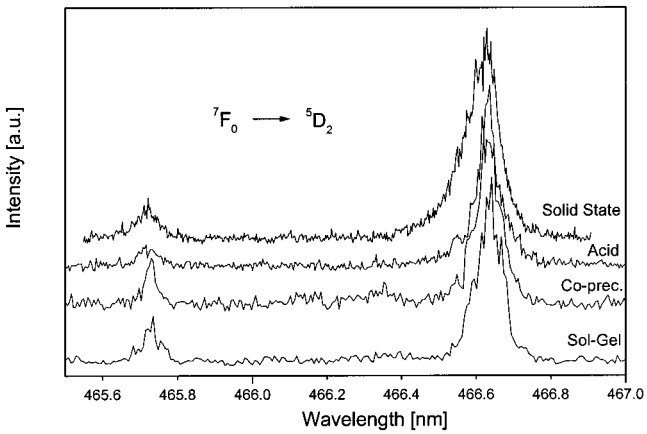

Figure 5. Excitation spectra recorded for the $^7F_0 \rightarrow {}^5D_2$ transition for the different samples.

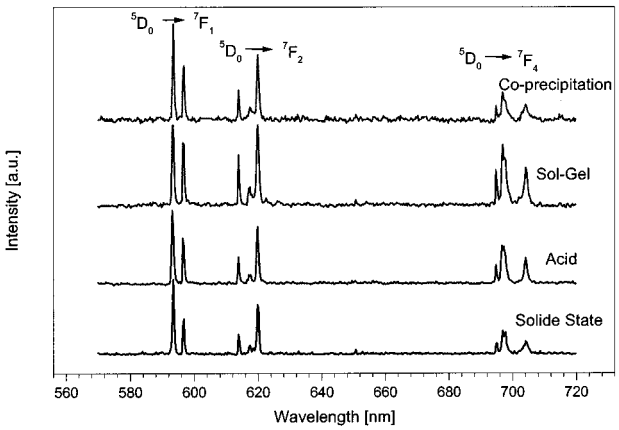

Figure 6. Emission spectra recorded after excitation in the $^5D_2$ level for the different samples.

$^5D_2$ level results in a different type of decay curve as shown in Figure 7b. These curves can be described as the sum of two exponentials with opposite signs. The short time raising component can be attributed to the population of the $^5D_0$ state from nonradiative desexcitation of the $^5D_2$ level. All curves were fitted with exponential functions. To model the decay curves obtained after blue excitation, the time constant determined from the fitting procedure of the decay obtained after excitation in the $^5D_0$ level was used for the long time component. Results of the fitting procedure are presented in Table 2.

Table 2. Lifetimes of the $^5D_0 \rightarrow {}^7F_2$ Transition for the Different Samples after Excitation in the $^5D_0$ and $^5D_2$ Levels Measured at 15 K

excitation		solid state	coprecipitation	acidic attack	sol−gel
$^5D_0$	τ_1 (ms)	3.4 ± 0.1	2.6 ± 0.1	2.9 ± 0.1	2.7 ± 0.1
$^5D_2$	τ_2 (μs)	38 ± 1	29 ± 1	31 ± 1	26 ± 1

Table 3. Relative Emission Efficiencies η for the Different Samples Doped with 5% Eu^{3+} and Compared to Y_2O_3:Eu^{3+} 4.47 mol % at Room Temperature after Excitation at 254 nm

	solid state	coprecipitation	acidic attack	sol−gel
η (%)	2.7 ± 0.1	6.0 ± 0.7	0.9 ± 0.1	0.4 ± 0.1

Emission Efficiencies. Relative emission efficiencies of the different phosphors have been measured by comparison with commercial Y_2O_3:Eu^{3+} 4.47 mol %. At this point, it is worth noting that the excitation (λ = 254 nm) does not correspond to the actual wavelength used in plasma systems and it is well-known that extrapolations are meaningless. Nevertheless, these measurements provide a good evaluation of the influence of the synthesis procedure on the luminous efficiency of the material.

Relative efficiencies toward the Y_2O_3 reference are gathered in Table 3. All measurements were performed at room temperature. Classification of the different phosphors according to their emission efficiency: coprecipitation > solid state > acid > sol−gel.

Discussion

It is clear from XRD and NMR measurements that all synthesis pathways lead to pure YPO_4 and that doping with Eu^{3+} at 5% does not affect the xenotime structure.

XRD measurements and SEM pictures demonstrate how liquid routes allow the control of the morphology

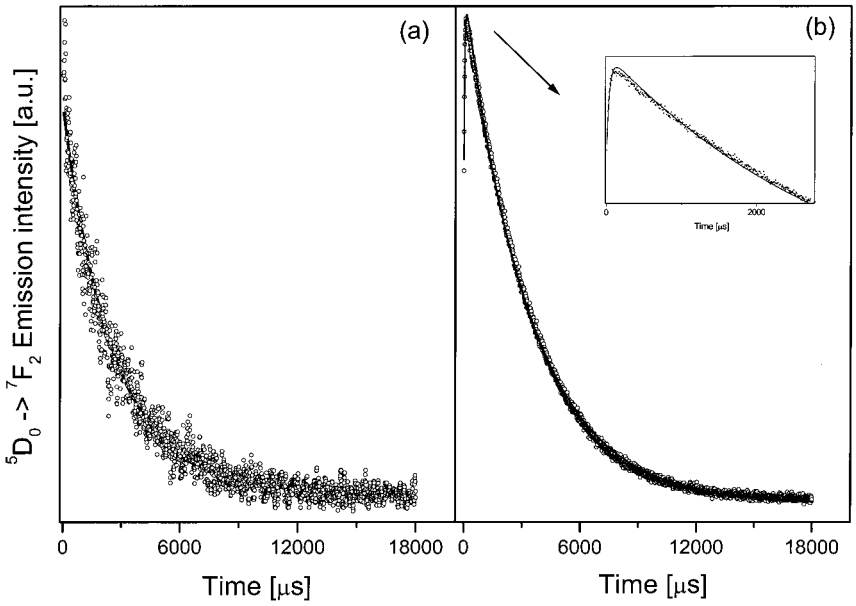

Figure 7. Typical decay curves obtained for the $^5D_0 \rightarrow {}^7F_2$ transition after excitation in the $^5D_0$ (a) and $^5D_2$ (b) levels.

of the polycrystalline powders. From the results obtained, the sol−gel process appears to provide the smallest particles with the narrowest size distribution. This control over the powder morphology is very important since the luminescent properties are strongly dependent on the powder granularity. Furthermore, for applications such as lamps and screens, where the phosphor is applied as a layer, narrow size distribution is strongly desirable to achieve homogeneous devices and lower the cost by decreasing the amount of matter deposited.

On another hand, optical measurements show that all samples present the same energetic scheme with similar excitation and emission spectra. Numbering of the emission lines for the different transitions is fairly well in agreement with the D_{2d} symmetry of the Y site in YPO_4, which is also the point group for substituting Eu^{3+} ions. Indeed, two $^5D_0 \rightarrow {}^7F_1$, three $^5D_0 \rightarrow {}^7F_2$, and three $^5D_0 \rightarrow {}^7F_4$ transitions are mainly observed and the shoulders observed on the main emission peaks probably indicate a small deviation from the ideal D_{2d} symmetry. This observation can be correlated to the difference between the crystallographic structures of YPO_4 and $EuPO_4$ which results in a slight distortion of the D_{2d} site upon doping with Eu^{3+} ions.

Nevertheless, the specific spectral signature[14] of the monazite type $EuPO_4$ is never observed in our experiments confirming that the distortion is small.

Lifetime measurements indicate a shorter lifetime for the $^5D_0 \rightarrow {}^7F_2$ emission in materials derived from liquid routes when compared to the solid-state material. This fact can be easily explained by invoking residual OH groups in soft chemistry derived materials. It is well-known[15,16] that liquid routes, and in particular the sol−gel process in which metal hydroxide intermediates are formed, yield materials with residual hydroxyl groups. These hydroxyl groups behave as very efficient quenchers of the luminescence via nonradiative desexcitation processes due to their high-energy vibration mode ($\sim$3500 cm^{-1}). Existence of these residual OH groups explains both the shorter lifetimes observed for liquid routes derived samples and the low emission efficiency measured for the sol−gel samples. For the reasons stated above, the sol−gel derived material undoubtedly has the larger concentration of residual OH groups. It is then very interesting to note that the coprecipitated sample, even if we can suggest some residual OH groups (see the emission lifetime), shows an emission efficiency that is more than twice that of the solid-state sample. It appears from these measurements that the appropriate soft chemistry route to phosphors can enhance their luminescence.

In conclusion, this work has shown that liquid routes can afford a control of both morphology and luminescent properties of YPO_4-based phosphors. The sol−gel process appears to be the most suitable to obtain small particles with a narrow distribution, and the coprecipitation provides phosphors with improved emission efficiencies. These preliminary results are somewhat encouraging, and improvement and optimization of the conditions of synthesis could lead to even better results in terms of grain size and luminous efficiency. The considerations used for YPO_4 phosphors should be extended to other various oxide phosphors. Furthermore, the sol−gel process offers a unique low-cost solution (dip-coating or spin-coating) to the production of high optical quality luminescent thin films,[17−19] which are very attractive solutions for screens and lamps. Viability of the sol−gel process developed in this work for the production of YPO_4 thin films is currently under study.

Acknowledgment. Dr. D. Boyer is gratefully acknowledged for his assistance during the preparation of the sol−gel samples.

CM010572Y

(14) Dexpert-Ghys, J.; Faucher, M. D.; Mauricot, R. *J. Lumin.* **1996**, *69*, 203.
(15) Frey, S. T.; Horrocks, W. *Inorg. Chim. Acta* **1995**, *229*, 383.
(16) Bouajaj, A.; Ferrari, M.; Montagna, M.; Moser, E.; Piazza, A.; Campostrini, R.; Carturan, G. *Philos. Mag. B* **1995**, *71*, 633.
(17) Hirano, S.; Yogo, T.; Kikuta, K.; Sakamoto, W.; Koganei, H. *J. Am. Ceram. Soc.* **1996**, *79*, 3041.
(18) Nedelec, J. M.; Turrell, S.; Douay, M.; Bouazaoui, M. *J. Sol.-Gel Sci. Technol.* **2001**, *20*, 287.
(19) Urlacher, C.; Marco de Lucas, C.; Bernstein, E.; Jacquier, B.; Mugnier, J. *Opt. Mater.* **1998**, *12*, 19.